

Single-phase Inertial Factor: Laboratory vs. Field Measurements

MAHMOUD JAMIOLAHMADY and MEHRAN SOHRABI
Institute of Petroleum Engineering, Heriot-Watt University
Riccarton, Edinburgh, EH14 4AS, SCOTLAND, UNITED KINGDOM

Jami.Ahmady@pet.hw.ac.uk, Mehran.Sohrabi@pet.hw.ac.uk, <http://www.pet.hw.ac.uk>

Abstract: - Single-phase inertial factor, β , also known as non-Darcy factor, which is an important flow parameter for determining the productivity of gas wells, is either determined in laboratory or by analysing variable rate well test data. In this study β measurement on a Clashach core sample was conducted in the Laboratory. This β value was then used as an input flow parameter in the in-house finite-element based simulator. The simulator was employed to simulate a variable rate test for an open-hole and a perforated well completion. The results of the generated synthetic data were analysed to obtain the corresponding field β value under different field conditions. The results indicated that for the case of pure radial flow, open-hole, in a homogenous porous medium, β value from field data could be used. However, in the case of presence of any non-uniformity in the flow path, e.g., perforated completion, immobile water, heterogeneity, damage, layering, etc., the calculated β will also reflect these effects and is not necessarily the true representative of real β . The mechanisms of high-velocity flow effect reflected by β value is discussed to explain this difference.

Key-words: - Inertial factor, Non-Darcy flow, Velocity, Perforated completion, Compressible gas.

1 Introduction

In flow of fluids through a porous medium at low and moderate rates, the pressure gradient in the direction of flow is proportional to the fluid velocity. The mathematical statement for this relationship is Darcy's Law. At higher flow rates, in addition to the viscous component there is an extra pressure drop over that predicted by Darcy's law. As early as 1901 Forcheimer [1] recognised this effect and suggested that a second order non-linear term is needed in the flow equation to account for the additional pressure drop as,

$$\frac{dP}{dL} = \frac{\mu}{k} V + \beta \rho V^2 \quad (1)$$

where P is pressure, L is length, V is velocity, μ is viscosity, k is absolute permeability, ρ is density and β is single-phase inertial factor.

This equation could be described as the general flow equation, in that it represents both the Darcy and the non-Darcy flow regimes. When the flow is within Darcy's flow regime the second term on the right hand side approaches zero and the equation reverts back to Darcy's equation. A wide range of opinion exists in the literature on the mechanisms of this high-velocity flow effect, also known as non-Darcy or inertial effect [2] but we believe it can mainly be attributed to two mechanisms:

- (a) the convective acceleration and deceleration of fluid particles as they travel through the pores.
- (b) the irregular, chaotic flow of a fluid that results in random velocity fluctuations and mixing, which is known as turbulent flow.

For a given pressure drawdown the velocity of gas is much greater than that of oil because of its low viscosity. Therefore, the high velocity component in Equation 1 is generally included in equations describing the flow of real gas through porous medium and is omitted from liquid flow equations, which fall within creeping flow regime. However if there is a large pressure gradient especially around the wellbore then the inertial term could be significant even for the flow of liquid.

β value is either determined in laboratory or by analysing variable rate well test data. The β values obtained by these two methods are usually different for the same porous medium. In this study β measurement on a Clashach core sample was conducted in the laboratory. This β value was then used as an input flow parameter in the in-house finite-element based simulator. The simulator was employed to simulate a variable rate test for an open-hole and a perforated well completion. The results of the generated synthetic data were analysed to obtain the corresponding field β value under different field conditions. The β value obtained in Laboratory were compared with corresponding field values with some important conclusions. The mechanisms of high-velocity flow effect reflected by β value is discussed to interpret these findings.

2 Laboratory Measurement of Single-phase Inertial Factor

The determination of the single-phase β -factor in core laboratory is a relatively straightforward task. Under selected test conditions of pressure, temperature, gas type, etc., gas is flowed through a core at incremental flow rates. For each increment of flow rate the pressure difference across the core is measured.

Equation 1 for liquids suggests that a plot of $-\frac{dP}{dL}$ vs. $\frac{\rho v}{\mu}$ should yield a straight line of

which the slope is equal to β and the intercept is the inverse of permeability. However, this procedure cannot be followed for gases, as the density is not independent of pressure. The real gas law can be used to relate density to pressure as,

$$PV = znRT \quad \Rightarrow \quad \rho = \frac{M_w P}{zRT} \quad (2)$$

where M_w is Molecular weight of the gas, z is compressibility factor, R is gas constant and T is temperature. All the parameters in the equations presented here and implemented in the simulator are in consistent (SI) units. However, throughout the report some of the parameters are reported in field units for convenience (e.g., pressure in psia instead of Pascal).

To obtain the extended form of Forchheimer equation for steady state flow of gas in a core one can multiply Equation 1 by density, substitute from Equation 2 on left hand side and replace the ρv product, mass flow rate per unit area, on the right hand side by the term W/A , which is constant for linear flow through the core. Integrating the resultant equation, neglecting the variation of μ and z with pressure, gives:

$$\frac{M_w (P_1^2 - P_2^2) A}{2zRT\mu L W} = \frac{W}{A\mu} \beta + \frac{1}{k} \quad (3)$$

Now a plot of $y = \frac{M_w (P_1^2 - P_2^2) A}{2zRT\mu L W}$ versus

$x = \frac{W}{A\mu}$ gives a straight line with slope of β and

intercept of $1/k$. An example for the determination of β from experimental data for the Clashach core with $S_{wi} = 0.0\%$ and $k=553$ mD is shown in Figure 1. For this experiment the in-house high-pressure core flood facility was used to flow Methane gas at different high flow rates through a Clashach core sample with length of 0.66 m, diameter of 0.05 m, permeability of 553 mD and porosity of 0.1776. More information about experimental procedure

can be found elsewhere [3]. The viscosity and density of methane at the average test pressure of 13.8 Mpa (2000 psia) are $1.6E-5$ Pa.s and 100.3 kgm^{-3} .

3 Field Measurement of Single-phase Inertial Factor

Similarly to what went for the steady state flow of gas in a core, the extended form of Forchheimer equation for flow of gas in radial system can be obtained by integrating Equation 1 from any radius to the wellbore radius. However it should be noted that during this integration process area is not constant and is expressed by $A=2\pi rh$. The radial form of Equation 1 is:

$$\frac{dP}{dr} = \frac{\mu}{k} \frac{Q}{2\pi rh} + \beta \rho \left(\frac{Q}{2\pi rh} \right)^2 \quad (4)$$

where, r is radius, Q is volumetric flow rate and h is thickness.

Multiplying Equation 4 by density, substituting from Equation 2 on left hand side and noting that the ρQ product on the right hand side is mass flow rate, W , which is a constant, gives:

$$\frac{kM_w P}{\mu zRT} dP = \frac{W}{2\pi h} \frac{dr}{r} + \left(\frac{k}{\mu} \right) \frac{\beta W^2}{(2\pi h)^2} \left(\frac{dr}{r^2} \right) \quad (5)$$

Integrating Equation 5, neglecting the variation of μz product and μ with pressure, gives:

$$\frac{P_{ext}^2 - P_w^2}{2} = \left(\frac{\mu zRT}{kM_w} \right) \times \left[\frac{W}{2\pi h} \ln \left(\frac{R_{ext}}{R_w} \right) + \left(\frac{k}{\mu} \right) \frac{\beta W^2}{(2\pi h)^2} \left(\frac{1}{R_w} - \frac{1}{R_{ext}} \right) \right] \quad (6)$$

The flow-rate of a gas well is conventionally expressed in volumetric rate at standard conditions, which is really a measure of mass flow rate. If mass flow rate is expressed in terms of flow rate at standard conditions, Q_{sc} Equation 6 takes the following form:

$$P_{ext}^2 - P_w^2 = \left(\frac{\mu zRT}{kM_w} \right) \left(\frac{2\rho_{sc} Q_{sc}}{2\pi h} \right) \left[\ln \left(\frac{R_{ext}}{R_w} \right) + \left(\frac{k}{\mu} \right) \frac{\beta (\rho_{sc} Q_{sc})}{(2\pi h)} \left(\frac{1}{R_w} - \frac{1}{R_{ext}} \right) \right] \quad (7)$$

where subscript (sc) refers to the value of quantity at standard conditions.

Using ideal gas law for ρ_{sc} , Equation 2 for $z=1$, results in:

$$P_{\text{ext}}^2 - P_w^2 = \left(\frac{P_{\text{sc}}}{\pi T_{\text{sc}}} \right) \left(\frac{\mu z T Q_{\text{sc}}}{kh} \right) \left[\ln \left(\frac{R_{\text{ext}}}{R_w} \right) + \left(\frac{k}{\mu} \right) \left(\frac{M_w P_{\text{sc}}}{RT_{\text{sc}}} \right) \times \left[\frac{\beta(Q_{\text{sc}})}{(2\pi h)} \left(\frac{1}{R_w} - \frac{1}{R_{\text{ext}}} \right) \right] \right]. \quad (8)$$

Assuming $1/R_w \gg 1/R_{\text{ext}}$ gives:

$$P_{\text{ext}}^2 - P_w^2 = C_{19} \left[\ln \left(\frac{R_{\text{ext}}}{R_w} \right) + D Q_{\text{sc}} \right] \quad (9)$$

$$C_{19} = \left(\frac{P_{\text{sc}}}{\pi T_{\text{sc}}} \right) \left(\frac{\mu z T Q_{\text{sc}}}{kh} \right)$$

with D defined by

$$D = \left(\frac{k M_w \beta}{\mu h R_w} \right) \left(\frac{P_{\text{sc}}}{RT_{\text{sc}} 2\pi} \right). \quad (10)$$

The assumption of $\mu z = \text{constant}$ is not always a realistic and can be avoided by the use of pseudo-pressure first proposed by Al-Hussainy et al. [4] as,

$$\psi(P) = \int_{P_b}^P \frac{\rho}{\mu} dP \quad (11)$$

where P_b is a low base pressure value.

The advantage of $\psi(P)$ is that it can be computed in advance by knowing the variation of density and viscosity with pressure. Substituting ρ from Equation 2 in 11, an equation similar to that of Equation 9 is obtained as

$$\psi(P_{\text{ext}}) - \psi(P_w) = C_{20} \left[\ln \left(\frac{R_{\text{ext}}}{R_w} \right) + D Q_{\text{sc}} \right]. \quad (12)$$

$$C_{20} = \left(\frac{P_{\text{sc}}}{\pi T_{\text{sc}}} \right) \left(\frac{T Q_{\text{sc}}}{kh} \right)$$

It should be noted that although in pseudo pressure analysis the variation of μz product with pressure has been accommodated inside the definition of pseudo-pressure but the value of viscosity appearing in the definition of D is assumed to be constant.

3.1 Skin Concept

The steady state radial flow of a single incompressible phase into an un-perforated open hole well is calculated by

$$Q_{\text{OH}} = \frac{2\pi kh}{\mu} \left(\frac{(P_{\text{ext}} - P_w)}{\ln(R_{\text{ext}}/R_w)} \right) \quad (13)$$

where subscript (OH) refers to open hole completion.

The common practice in the well performance engineering is to account for any non-uniformity in flow compared to that of radial open hole using skin concept [5]. That is, the steady state flow into a perforated well for the same pressure drop is described by

$$Q_p = \frac{2\pi kh}{\mu} \left(\frac{(P_{\text{ext}} - P_w)}{\ln(R_{\text{ext}}/R_w) + S} \right) \quad (14)$$

where S is the skin factor, corresponding to a dimensionless pressure drop assumed to occur at the wellbore face as a result of a damage ($S > 0$) or improvement ($S < 0$) around the wellbore compared to radial open hole, i.e., Equation 13. Subscript (p) refers to perforated completion.

In the case of compressible gas pseudo-pressure instead of pressure and mass flow rate instead of volumetric flow rate is used [4] as,

$$m_p = 2\pi kh \left(\frac{\psi(P_{\text{ext}}) - \psi(P_w)}{\ln(R_{\text{ext}}/R_w) + S} \right). \quad (15)$$

The advantage of $\psi(P)$ is that the compressible gas equations preserve similarity to the incompressible single-phase equations and all concepts relating to skin is immediately applicable.

The high velocity component is also considered as an additional skin factor, resulting in an additional pressure drop. Therefore, it is considered that total skin, S_T , for a gas well consists of two components laminar component, S, and the non-Darcy component, DQ, defined as,

$$S_T = S + D Q_{\text{sc}}. \quad (16)$$

Comparing Equation 16 with 15, Equation 12 can be re-written as,

$$\psi(P_{\text{ext}}) - \psi(P_w) = C_{20} \left[\ln \left(\frac{R_{\text{ext}}}{R_w} \right) + S_T \right]. \quad (17)$$

Equation 16 states that S_T of a gas well is not constant and varies with flow rate. This means that some form of variable rate test is essential so that the two components of S_T can be decomposed. There are different types of tests proposed for this purpose, which can be divided into two main categories, i.e., stabilized and transient tests. In the first category, e.g., Flow-after-flow test or Isochronal test, the bottom hole flowing pressure apparently reaches stabilisation towards the end of each flow period to enable one to use a time independent equation similar to that of Equation 17 to describe the flow of gas. In the second category, e.g., step-rate transient (SRT), a time dependent solution describes the flow of gas similar to the classic solution of diffusivity equation, which is beyond the scope of the present discussion and more information can be found elsewhere [5].

However, in all these tests the skin factors are obtained at different rates and assuming Equation 16 is valid the slope of the best-fit-straight line through Q vs. S_T plot is the optimal estimate of non-Darcy coefficient, D , and the intercept at $Q=0$ is the original estimate of the Darcy skin S . The D value obtained following this procedure is then used to calculate the inertial factor, β , using Equation 10.

As mentioned earlier in this study to replicate filed β measurement procedure discussed above we generated some synthetic data using the in-house single-well simulator. In this exercise the steady state flow of compressible fluid including inertia into an open hole and a perforated completion was simulated. Here we present some of the key features of the models but more information can be found elsewhere [6,7].

3.2 Structure of Single-well Models

The 3-D perforated well model considered in this study consists of a well with the radius of R_w in a single layer cylindrical reservoir with the external radius of R_{ext} , Figure 2. It is a homogenous porous medium with an absolute permeability k and the formation thickness of h . The cylindrical perforation tunnels with the radius R_p and the length of L_p are distributed spirally around the wellbore with a shot density of SPF, which refers to the number of perforation tunnels per foot. Angular phasing, ϕ , denotes the angle between two successive perforation tunnels and its value is constant. The values of SPF and ϕ in Figure 2 are 4 and 90° , respectively.

The 1-D open-hole well model, used in this study, consists of a well with radius of R_w in a single layer cylindrical reservoir with external radius of R_{ext} . The 1-D model uses the existing symmetry in z and angular direction for this radial flow pattern. The other features of 1-D model are similar to those of the 3-D model.

4 Results

Different pressure drops were applied across the drainage area and the skin values, corresponding to additional pressure drop caused due to the presence of perforation &/or inertia compared to open hole well, Darcy flow regime, were calculated using Equation 15 at each flow rate. In these simulations the wellbore diameter, D_w , is 8.625 inches and external radius, R_{ext} , is 60 times R_w . The pressure difference across the flow domain from R_{ext} to R_w has been 0.16, 0.5, 1, 2.5, 5, 10, 20, 50, 100, 400 psi with $(P_{ext}+P_w)/2=1565$ psia.

Figure 3 shows the plot of total skin versus well flow rate for a radial open hole completion and five different perforation lengths of a 4 SPF perforated completion with 0° phasing angle. The data of Figure 3 clearly demonstrates the dependency of D on perforation length as the slope of fitted straight line is different for the open hole completion compared to that of the perforated ones and varies for different perforation length values. Table 1 gives the calculated values of β using Equation 10. It is noticed that in this table all the β values corresponding to perforated completion are greater than the corresponding value measured in the core laboratory. However, the β value obtained for the radial open hole completion is almost equal to that of core laboratory with AD% of 2.2%, which is in the range of accuracy of the simulations. This is due to the fact that the change in flow path as a result of a change in perforation arrangement results in different share for inertia compared to what has been considered in the derivation of Equation 10, which is only valid for the case of open-hole.

Figure 4 displays the plot of total skin versus well flow rate at five different perforation lengths for the same 4SPF perforation geometry but with 90° degree phasing angle. Similarly to Figure 3 the data of open hole completion is also included in this Figure. The same observation as that of Figure 3 can be made whereby the fitted straight lines have different slope. However, the β values calculated for these different D values exhibit a different trend compared to those for zero degree phasing discussed earlier, Table 1. In the former the β value at perforation length of 15 inches is lower than the corresponding value measured in the core laboratory whilst for the latter it was higher at all L_p values. The difference between these two cases is that in the former there is a larger improvement due to perforation operation, which suggests that the effect of inertia is yet to become dominant whilst for the latter under the applied pressure differences the inertial effect is more dominant compared to that of open hole situation due to more pronounced flow convergence.

The dependency of β to perforation characteristics and arrangements suggests that the presence of any non-uniformity in the flow path compared to that of open-hole in a homogenous porous medium, which results in a different share of inertia compared to that considered in the derivation of Equation 10, makes the result of field β measurement different from the β value measured in the core laboratory.

5 Conclusions

The single-phase inertial flow resistance factor, β is a fundamental rock property as determined in core laboratory. The common practice in the well performance engineering is to include the high velocity flow component as an additional skin factor, resulting in an additional pressure drop compared to that of pure radial open hole Darcy flow regime. Based on this concept field data from a variable rate test is used for the prediction of β .

We investigated the validity of this procedure by generating some synthetic field data for steady state simulation flow of gas into an open hole and a perforated completion using the in-house finite-element based simulator. The results presented here indicated that the field β measurement for an open hole completion matches that of core laboratory for a homogenous undamaged case. However for majority of perforated completion the field β is either higher or lower than laboratory β , depending perforation characteristics and arrangements. Therefore, it can be concluded that the presence of any non-uniformity in the flow path compared to that of open-hole in a homogenous porous medium, which results in a different share of inertia compared to that considered in the derivation of Equation 10, makes the result of field β measurement different from the β value measured in the core laboratory. Hence, care should be taken in the analysis of the field data and its correct implementation in later field life calculation.

ACKNOWLEDGEMENTS

The above study has been sponsored by: The UK Department of Trade and Industry, BP Exploration Operating Company Ltd, Gaz de France, Marathon Oil UK, Statoil A.S.A. and Total Exploration UK plc, which is gratefully acknowledged.

REFERENCES

[1] Forchheimer, P.: *Hydraulik*, 1914, Chapter15, pp. 116-8, Leipzig and Berlin.

[2] Al-Kharusi, B.: *Relative permeability of gas condensate near wellbore, and gas-condensate-water in bulk of reservoir*”, PhD Thesis, Institute of Petroleum Engineering, Heriot-Watt University, January 2000, Appendix 2.

[3] Jamiolahmady, M., Danesh, A, Sohrabi, M. and Duncan, D. B., *Flow around a rock perforation surrounded by crushed zone: Experiments vs. Theory*, 2005, accepted for publication in *J. Petrol. Sci. Engng.*

[4] Al-Hussainy, R. and Ramey, H. J., Jr., *The Flow of Real Gases Through Porous Media*, *J. Pet. Tech.*, May 1966, pp. 624-636.

[5] Earlougher, R.C.: *Advances in well test analysis*, *American Institute of Mining, Metallurgical and Petroleum Engineers (AIME)*, 1977.

[6] Jamiolahmady M. and Danesh A.: “Flow in Perforated Region Including Non-Linear Effects,” *Proceedings of the 67th EAGE Conference and Exhibition, Spain, June 2005.*

[7] Jamiolahmady M., Danesh A. and Sohrabi M.: *Gas Condensate Flow in Perforated Region*, SPE 94072, *Proceedings of the SPE Europec Conference, SPE 94072, June 2005.*

Table 1: skin and single-phase inertial factor values calculated from gas production data of an open hole completion and a 4SPF perforated completion at five perforation lengths and two phasing angles. The porous medium is Clashach with $k=553$ mD and $\beta=1.035E8$ m⁻¹.

L _p /inch	0-degree phasing		90-degree phasing	
	$\beta*1E-8$ /m ⁻¹	Skin	$\beta*1E-8$ /m ⁻¹	Skin
3	15.558	3.33	12.765	1.87
6	5.729	1.92	3.970	0.6
9	3.350	1.27	2.044	0.29
12	2.278	0.84	1.338	-0.03
15	1.725	0.54	0.952	-0.06
Open Hole	1.012	0.02	1.012	0.02

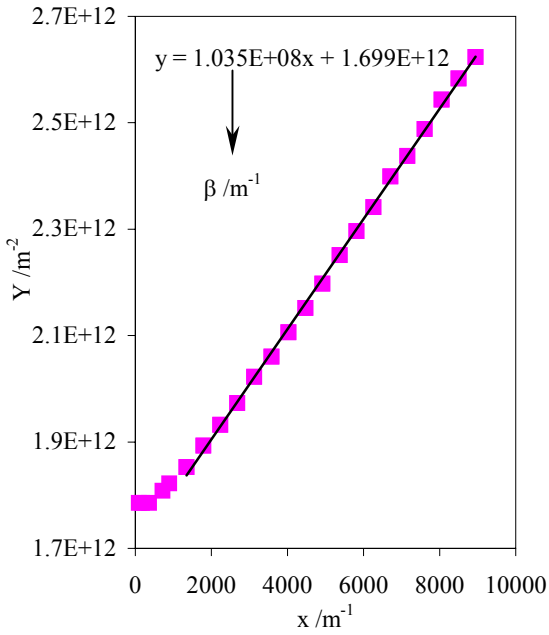


Figure 1: Laboratory beta measurement for Clashach core, $S_{wi}=0.0\%$, $k=553$ mD, Equation 3.

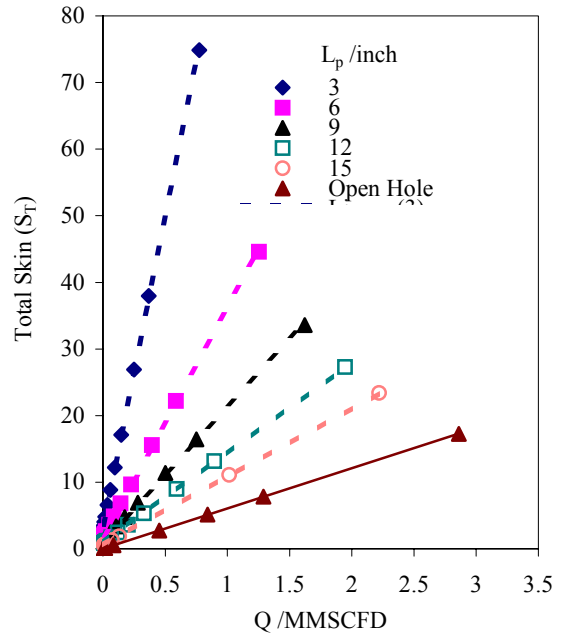


Figure 3: Total skin versus well flow rate for a radial open hole completion and five different perforation lengths of a 4 SPF perforated completion with 0 degree phasing angle.

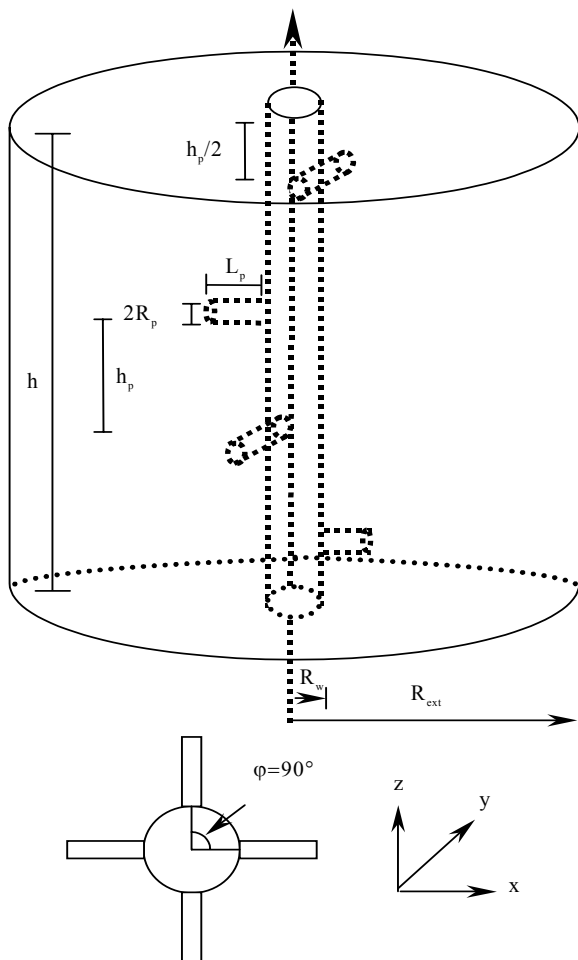


Figure 2: A perforated region with four shots per foot and 90 degree phasing angle.

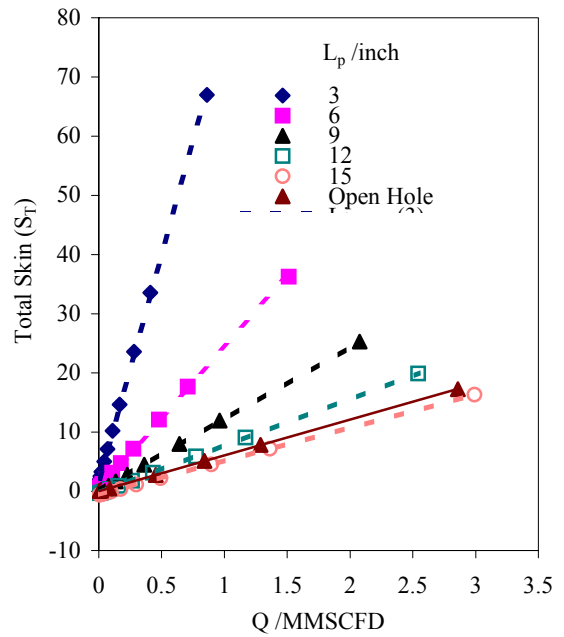


Figure 4: Total skin versus well flow rate for a radial open hole completion and five different perforation lengths of a 4 SPF perforated completion with 90 degree phasing angle.